

RANDOM COEFFICIENT DIFFERENTIAL MODELS OF GROWTH OF ANAEROBIC PHOTOSYNTHETIC BACTERIA*

DAN STANESCU[†], BENITO CHEN-CHARPENTIER[‡],
BRANDI J. JENSEN[§], AND PATRICIA J. S. COLBERG[¶]

Abstract. In many fields of science and engineering there are mathematical models given in terms of differential equations with random coefficients. The randomness is due to errors or uncertainty. Closed solutions are few, and usually numerical approximations need to be calculated. Polynomial chaos is a powerful method in this regard. Here we apply this method to several modeling approaches for the time evolution of photosynthetic bacterial populations. Usual methods used in microbiology are contrasted with approaches based on differential equations with random coefficients. Numerical results based on laboratory data for two different species of bacteria are presented.

Key words. bacterial growth models, random differential equations, curve fitting

AMS subject classifications. 60H25, 65C20, 92D25

1. Introduction. Differential equations with random coefficients are used as models in many different applications. In many situations they are better in describing the real behavior than equations with deterministic coefficients because of errors in the observed or measured data, because of variability of the conditions, and also because of uncertainties or lack of knowledge. Uncertainty can be due to variables that cannot be measured and also to missing data. Random differential equations have been used in the last few decades to deal with errors and uncertainty. For example see [17] and [13]. Another method of dealing with uncertainty and errors is to add an additive or multiplicative noise term to the equation; see, for example, [7] and [13].

The most well known methods to work with random coefficient differential equations are the Monte Carlo method, moment methods, and polynomial chaos.

1. Monte Carlo. In this approach (see, for example, [11] and [3]), the basic procedure is:

- Generate sample values of the random variable(s) from their known or assumed probability density function.
- Solve the deterministic equation corresponding to each value.
- Calculate statistics, such as mean and variance, of the set of deterministic solutions.

This method is straightforward, but very expensive since it requires many realizations.

2. Method of Moments. This method is based on obtaining the moments of the solution, usually only the mean and variance; see, for example, [5] and [16]. Usually expansions in terms of a small random term about a deterministic coefficient or mean square calculus are used. Soong [16] applied the method to a Malthus growth population model and Villafuerte [19] extended it to the logistic growth model.

*Received March 31, 2008. Accepted October 7, 2008. Published online March 31, 2009. Recommended by Godela Scherer.

[†]Department of Mathematics, University of Wyoming, Laramie, WY 82071 (stanescu@uwyo.edu).

[‡]Department of Mathematics, University of Texas at Arlington, Box 19408, 439 Pickard Hall, Arlington, TX 76019 (bmchen@uta.edu).

[§]Department of Zoology and Physiology, University of Wyoming, Laramie, WY 82071 (bjensen@uwyo.edu).

[¶]Department of Civil and Architectural Engineering, University of Wyoming, Laramie, WY 82071 (pczoo@uwyo.edu).

3. Polynomial Chaos. The method will be described and applied to population growth models in Section 4.

In the life sciences, a very important field of study is that of population growth and evolution of organisms with time. Field observations and laboratory experiments are often performed to determine the sizes of different types of populations under varying conditions and their changes with time. To be able to extend the results to other situations and to make predictions, mathematical models are needed. These models involve parameters, such as the rate of growth, that are usually determined from the measurements of the population size by some sort of curve fitting. Two population models widely used are exponential growth, or Malthusian growth, and logistic growth.

Even when the measurements are done with the utmost care, the measured values will differ somewhat; in fact, sometimes the variability is quite dramatic. This is due to inaccuracies in the methods used to assess population size, error (human or otherwise), and variability in the populations, as well as other unknown factors; in reality, what one obtains are parameters that have some variation. The initial value of the population can also have variations, but these are due only to errors in their measurement. As previously mentioned, a new way to deal with the variation of the parameters is to consider them to be random variables with a specified, given distribution.

In this paper, we will use actual laboratory data from the growth of anaerobic photosynthetic bacteria under infrared lighting conditions. These organisms use light energy to reduce CO₂ and synthesize carbohydrates, which simultaneously results in an increase in biomass. Initially, when there is no competition for light and/or CO₂, the growth may be modeled with an exponential growth model. Later, as the population increases in size, the access to light and/or CO₂ is reduced; the experimental values can now be better fitted using a logistic model. (One of the data sets fits very well an 's-curve' given by a logistic growth model. The second data set has two points where, for unknown reasons, the population appears to have decreased. So we do not expect the models to fit very well for these data.) We will consider that the fitted parameters are random variables and will obtain the equations for the time evolution of their means and variances. We will then solve these equations and show the effects of the randomness on longer time predictions.

The rest of the paper is structured as follows. In Section 2, the biological problem of the growth of anaerobic photosynthetic bacteria is presented and the experiments described. In Section 3, the mathematical models with fixed parameters are introduced and the curve fitting procedure presented. In Section 4, the random models are discussed and in Section 5 numerical results pertaining to them are presented. Finally, Section 6 draws the conclusions.

2. Anaerobic photosynthetic bacterial growth. In this section, we briefly describe how the experiments to measure the population sizes of *Rhodobacter capsulatus* (*R. capsulatus*) and *Chlorobium vibrioforme* (*C. vibrioforme*) under infrared lighting conditions were performed.

Rhodobacter capsulatus (DSM 1710) and *Chlorobium vibrioforme* strain 6030 (DSM 260) were obtained from the Deutsche Sammlung von Mikroorganismen und Zellkulturen (DSMZ, Braunschweig, Germany). *Rhodobacter capsulatus* was grown in a medium proposed by Siström [15] and modified by Kessi et al. [8]. *Chlorobium vibrioforme* was grown in Medium 40 as recommended by the DSMZ.

All cultures were plated anaerobically to ensure culture purity before use. Plates were made using the specified medium plus 15 g/L Bacto-Agar (Difco Laboratories, Detroit, MI) and incubated in an anaerobic jar. Once pure cultures were insured, three tubes containing 20 mL of fresh media were inoculated with 1 mL of mature culture, meaning that pigmentation had been observed for two weeks. These tubes were allowed to grow anaerobically for two

weeks in light using three 60W tungsten incandescent light bulbs (Crystal Clear, ACE, Oak Brook, IL) at 21°C. Five tubes, each containing 20 mL of media, were then inoculated with 1 mL culture and placed in the dark for 12 hours. After the dark incubation period, the cultures were grown under anoxic conditions under infrared illumination.

Bulbs used for IR incubations were placed behind 58 mm R72 infrared glass filters (Hoya Corporation, Tokyo, Japan) that allowed wavelengths of light above 700nm to pass. All cultures were incubated between 21 – 23°C. Light intensity was measured using a Digital Lux Meter (LX-101A, Lutron, Taipei, Taiwan). *Rhodobacter capsulatus* was incubated at a light intensity of 60 lux; *C. vibrioforme* was provided 120 lux.

Direct cell counts were made using the Acridine Orange Method [9] and a Dialux 20 epifluorescence microscope fitted with a lens micrometer (Leitz, Germany). Fifteen to twenty fields were counted and averaged to determine the population size at any point in time. Cell numbers were assessed upon initial inoculation and then again when pigmentation was visible in the cultures. Cell counts were then made every two to three days until a stationary phase was achieved. The measured values are presented in the next section.

3. Mathematical models and curve fitting. If we let $y(t)$ be the population of a given species at time t , then the simplest model for the growth or decay of the population is that the rate of change is proportional to the size of the population. This is the model proposed by Thomas Malthus in 1798 [10, 12]. The differential equation for this model is

$$\frac{dy}{dt} = ry(t), \quad (3.1)$$

where r is the growth rate. The solution for an initial value of the population $y(0) = y_0$ is $y(t) = y_0 \exp(rt)$. For up to nine days, our bacteria populations have a growth rate that looks exponential.

But, of course, as the population keeps growing inside the test tubes, there starts to be a competition for the limited resources, mainly light and possibly CO₂. In 1838, Verhulst [18] proposed that the growth rate should decrease with the size of the population. This leads to the logistic equation

$$\frac{dy}{dt} = r \left(1 - \frac{y}{K}\right) y. \quad (3.2)$$

Here r is still the growth rate and K is the equilibrium value. The solution, subject to initial value $y(0) = y_0$, is

$$y(t) = \frac{y_0 K}{y_0 + (K - y_0) \exp(-rt)}.$$

Our data, for times up to 14 days, resembles logistic growth.

We will fit our experimental data to both exponential and logistic models using least squares. That is, we have a set of experimental values (t_i, y_{exp_i}) , $i = 1, \dots, m$, with m the number of data points, a set of parameters to fit, r_j , $j = 1, \dots, npar$, with $npar$ the number of parameters to fit, and a model for the size of the population $\mathbf{f}(\mathbf{r}, t_i)$, with \mathbf{f} a vector-valued function of dimension m and \mathbf{r} the vector of parameters of size $npar$. We want to find the values of \mathbf{r} that minimize

$$\psi(\mathbf{r}) = \sum_{i=1}^m (\mathbf{f}(\mathbf{r}, t_i) - y_{exp_i})^2;$$

TABLE 3.1
Cell counts.

<i>R. capsulatus</i>		<i>C. vibrioforme</i>	
Time	Population	Time	Population
(days)	(cells/mL)	(days)	(cells/mL)
0	5.83E+05	0	9.86E+05
2	6.35E+05	14	2.41E+06
4	1.08E+06	16	2.24E+06
7	3.20E+06	18	4.21E+06
9	5.23E+06	21	5.72E+06
11	5.28E+06	23	5.99E+06
14	5.30E+06	25	7.86E+06
		28	6.52E+06

see, for example, [2]. Since in the majority of cases, the model curve will not go through all the experimental points, the minimum value will not be zero. The final value of $\psi(\mathbf{r})$ gives a measure of how good the fit is. We will call this value the residual or the norm of the residual.

We will fit the parameters to our data in three ways. First (Case I), we will only use the data up to nine days, and fit only the growth rate parameter to the Malthusian model. Second (Case II), we will use the same data but also fit the initial value of the population to the same model. Finally (Case III), we will use all the data and fit the growth rate, the initial value and the equilibrium value using a logistic growth model.

In the process of fitting the parameters, y_0 and K are scaled by 10^6 to make all the parameters that are fitted to be of the same order.

Table 3.1 contains the measured population values for *R. capsulatus* and *C. vibrioforme* under IR lighting conditions. Figures 3.1–3.2 plot the measured values of the populations of *R. capsulatus* and *C. vibrioforme*, respectively, together with smooth cubic interpolation curves going through those values. The curves do not represent exponential or logistic (“s-shaped”) curves very well, but they give us a test case when we do not expect the curve fitting to be very good.

4. Random coefficients and polynomial chaos.

4.1. Exponential growth. To start with, let us consider the model ordinary differential equation

$$\frac{dy(t; \omega)}{dt} = r(\omega)y, \quad y(0; \omega) = y_0(\omega), \tag{4.1}$$

where the growth rate coefficient $r(\omega)$ as well as the dependent variable $y(t; \omega)$ for a given t are supposed to be random variables of the outcome of an experiment ω taking values in the set of all outcomes Ω . The latter is assumed to be properly equipped with a σ -algebra \mathcal{F} and a probability measure P such that the triple (Ω, \mathcal{F}, P) forms a probability space [14]. Moreover, the initial condition $y_0(\omega)$ and the growth rate are supposed to be independent random variables. For several types of distributions of the growth rate, the time evolution of the expected value of $y(t; \omega)$ can be obtained in closed form. In order to develop a more general methodology for the numerical solution of other evolution equations, we follow the polynomial chaos approach [4, 20, 22] using the Wiener-Hermite chaos expansion. In this

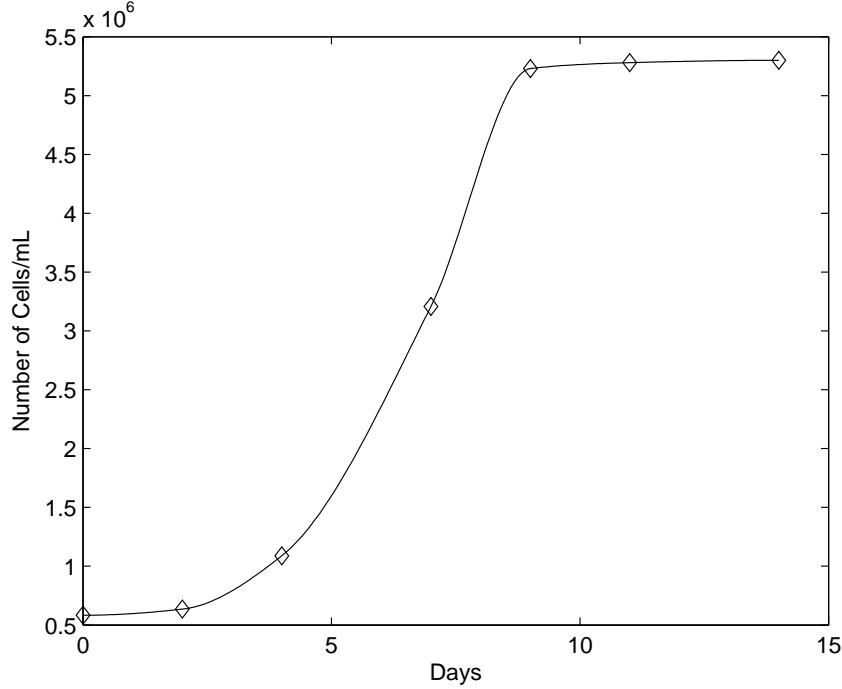


FIGURE 3.1. Population size of *R. capsulatus* versus time.

context, a random variable $\chi(\omega)$ is projected on the space of polynomial chaoses

$$\chi(\omega) = \chi_0 \Gamma_0 + \sum_{i_1=1}^{\infty} \chi_{i_1} \Gamma_1(\xi_{i_1}(\omega)) + \sum_{i_1=1}^{\infty} \sum_{i_2=1}^{i_1} \chi_{i_1 i_2} \Gamma_2(\xi_{i_1}(\omega), \xi_{i_2}(\omega)) + \dots, \quad (4.2)$$

where the Γ_i are successive polynomial chaoses of increasing degree in their arguments [21, 6, 4]. This expansion has been shown to converge for second-order random processes [1]. The polynomial chaoses can be arranged in a sequence $\Phi_i(\xi(\omega))$, such that the expansion of the random processes appearing in equation (4.1) takes the form:

$$y(t; \omega) = \sum_{i=0}^{\infty} y_i(t) \Phi_i(\xi(\omega)); \quad r(\omega) = \sum_{j=0}^{\infty} r_j \Phi_j(\xi(\omega)), \quad (4.3)$$

where the Φ_i are properly chosen polynomial basis functions of the random variable vector ξ . The number of variables in ξ represents the dimension of the chaos. We consider $\xi(\omega)$ a vector of standard Gaussian variables and take the basis functions to be the Hermite polynomials, leading to the Wiener chaos expansion. A Galerkin projection using the orthogonality of the basis functions $\langle \Phi_i, \Phi_j \rangle = \delta_{ij} \langle \Phi_i, \Phi_i \rangle$ together with truncation of the infinite series to $P + 1$ terms leads to a system of ordinary differential equations governing the time evolution of the chaos coefficients of the solution

$$\frac{dy_m}{dt} = \frac{1}{\langle \Phi_m, \Phi_m \rangle} \sum_{i=0}^P \sum_{j=0}^P a_{ijm} r_j y_i(t),$$

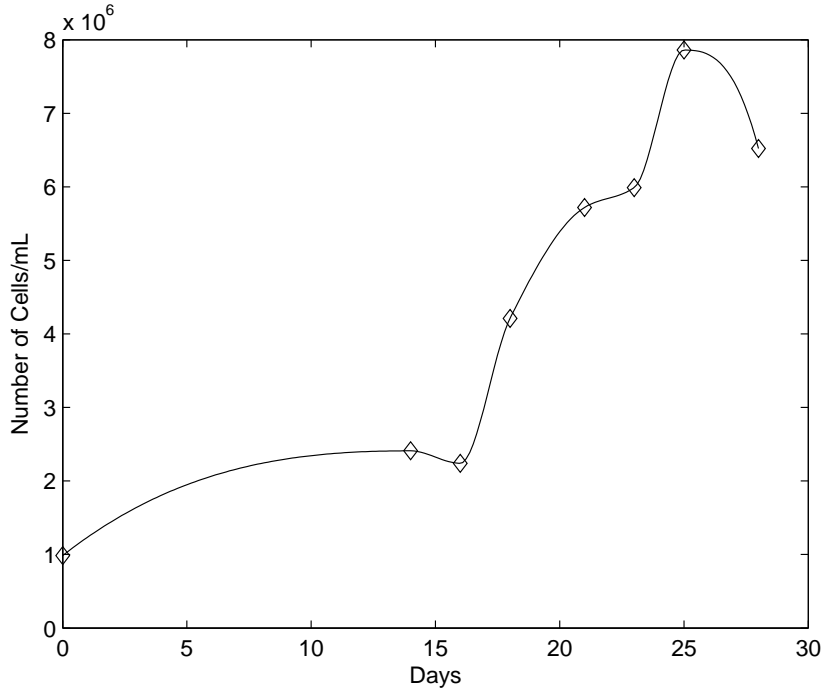


FIGURE 3.2. Population size of *C. vibrioforme* versus time.

where $a_{ijm} = \langle \Phi_m, \Phi_j \Phi_i \rangle$. This system is then integrated in time using an appropriate numerical method, and the chaos coefficients thus obtained can be subsequently used to compute quantities of interest. For example, the mean of y is the value of the first coefficient $y_0(t)$, while the variance of y is $\text{Var}[y] = \sum_{i=1}^P y_i^2(t) \langle \Phi_i, \Phi_i \rangle$. The inner product $\langle \cdot, \cdot \rangle$ in this paper is always taken with respect to Gaussian measure.

Some exact solutions for the expected values of the dependent variable in the case of this simple equation can be obtained. Since $y_0(\omega)$ and $r(\omega)$ are independent, from the exact solution of the equation (3.1) one obtains:

$$\bar{y}(t) = \bar{y}_0 E[\exp(rt)] = \bar{y}_0 \int \exp(xt) f_r(x) dx, \quad (4.4)$$

where \bar{y}_0 is the mean value of $y_0(\omega)$, $f_r(x)$ is the probability density function for the growth rate, and the integration should be performed over the support of f_r . If $r(\omega)$ is a Gaussian random variable with mean \bar{r} and variance σ_r^2 , then the integral can be evaluated exactly to give

$$\bar{y}(t) = \bar{y}_0 \exp\left(\bar{r}t + \frac{\sigma_r^2 t^2}{2}\right).$$

Similarly, for an exponential distribution of r , one obtains

$$\bar{y}(t) = \frac{\lambda \bar{y}_0}{\lambda - t},$$

where λ is the parameter of the exponential distribution, i.e., $\bar{r} = 1/\lambda$. For a uniform distribution of $r(\omega)$ in (a, b) , equation (4.4) leads to

$$\bar{y}(t) = \bar{y}_0 \frac{\exp(bt) - \exp(at)}{t(b-a)}.$$

These solutions have been used to confirm the numerical results obtained from the polynomial chaos implementation.

4.2. Logistic growth. The logistic growth equation (3.2) is considered here, in which the growth rate r and the equilibrium (or saturation) level K are random variables. Because of the nonlinear term in the logistic equation, it is known that moment methods are difficult to apply directly to (3.2) as they require closure for the higher-order moments. Moment methods based on sensitivities can be easily used because an exact solution is known [20]; however, in the case of differential equations where an exact solution is not available, these methods do require computation of sensitivities, usually a more complicated task than solving the differential equations. On the other hand, the polynomial chaos expansion is rather straightforward to apply. To develop the Galerkin projection of the solution on the polynomial chaos, and taking into account the fact that the saturation level K is necessarily positive, it is helpful to introduce $\kappa(\omega) = 1/K(\omega)$. Expanding this quantity in the polynomial chaos basis, similar to equation (4.3), and introducing the corresponding expression in equation (3.2), one obtains:

$$\sum_{i=0}^P y_i'(t) \Phi_i = \sum_{j=0}^P \sum_{i=0}^P r_j y_i(t) \Phi_j \Phi_i \left[1 - \sum_{k=0}^P \sum_{l=0}^P \kappa_k y_l(t) \Phi_k \Phi_l \right]. \quad (4.5)$$

Again taking the inner product with the basis function Φ_m , we obtain a system of ordinary differential equations for the time dependent coefficients in the solution,

$$\frac{dy_m}{dt} = \frac{1}{\langle \Phi_m, \Phi_m \rangle} \sum_{i,j=0}^P r_j y_i(t) a_{ijm} - \sum_{i,j,k,l=0}^P y_i(t) r_j \kappa_k y_l(t) b_{ijklm}, \quad (4.6)$$

with a_{ijm} as defined above and the additional coupling coefficient $b_{ijklm} = \langle \Phi_m, \Phi_i \Phi_j \Phi_k \Phi_l \rangle$. When the initial value y_0 and the reciprocal of the saturation level κ are deterministic, the exact solution for the first moment of $y(t; \omega)$ is given by

$$\bar{y}(t) = \int \frac{y_0 f_r(x)}{\kappa y_0 + (1 - \kappa y_0) \exp(-xt)} dx. \quad (4.7)$$

4.3. Random input representation. In most practical situations, a subset of the random coefficients in the model must satisfy constraints inherent to the model itself. For example, for the exponential growth model the initial population $y_0(\omega)$ has to be positive; no such constraint is necessary for $r(\omega)$, although negative values of r will lead to decrease of the population size in time. For the logistic model both $y_0(\omega)$ and $\kappa(\omega)$ must be positive. Obviously, normal random variables are not good candidates for the positive quantities, since they can take values all over the real axis. Thus, one needs to consider random variables whose probability density functions have support on the positive real axis. For this study we will only focus on uniformly distributed random inputs, although gamma, beta, and lognormal random inputs may be considered. To represent a non-Gaussian random input in a Hermite chaos expansion, one can use the inverse transform method [14] to map both the random variable which needs to be represented, say $r(\omega)$ with cumulative distribution function $F_r(x)$, and the standard normal random variables $\xi(\omega)$ to the same probability space. Given u uniformly

TABLE 5.1
Parameters for *R. capsulatus*.

	r	y_0	K	residual
Case I	.1762			1.8385
Case II	.2822	.4174E+06		.1206
Case III	.6157	.1244E+06	5.5623E+06	.600

TABLE 5.2
Parameters for *C. vibrioforme*.

	r	y_0	K	residual
Case I	.0774			2.2011
Case II	.1293	.3755E+06		1.0543
Case III	.3184	.0292E+06	7.4242E+06	3.3127

distributed in $(0, 1)$, the random variable $\rho(u) = F_r^{-1}(u)$ has the same distribution as r . The transformation is useful when F_r can be easily inverted. The inner products of $r(\omega)$ with the basis functions can then be computed by mapping to $(0, 1)$:

$$r_i = \frac{1}{\langle \Phi_i^2 \rangle} \langle r, \Phi_i \rangle = \frac{1}{\langle \Phi_i^2 \rangle} \int_0^1 F_r^{-1}(u) \Phi_i(F_r^{-1}(u)) du. \quad (4.8)$$

Another alternative, which we adopt here, is to map the uniformly distributed random variables in the interval $[a, b]$ to standard normals, in which case equation (4.8) for the case of one-dimensional chaos becomes

$$r_i = \frac{1}{\langle \Phi_i^2 \rangle} \left\langle a + (b - a) \frac{1 + \operatorname{erf}(\xi/\sqrt{2})}{2}, \Phi_i(\xi) \right\rangle. \quad (4.9)$$

5. Numerical experiments.

5.1. Deterministic model fitting. In this section we present the results of the curve fitting for the three cases and of numerical experiments with the various models presented above.

Case I refers to the results of fitting an exponential growth model to the measured data of *R. capsulatus* up to nine days, considering that the growth rate r is the only parameter to be fitted. For *C. vibrioforme*, the data fitted is up to 21 days. Since we are only fitting one parameter, the fit is not as good as in the other two cases.

Case II refers to the results of the curve fitting when the model is still growing exponentially, but we have two parameters, the growth rate r and the initial population y_0 . For *R. capsulatus*, the data used is up to nine days, and for *C. vibrioforme* it is up to 21 days.

Case III refers to the fit of a logistic model using all of the measured values. For *R. capsulatus*, the time is up to 14 days, and for *C. vibrioforme* it is to 28 days. Now we have three parameters to fit: the growth rate r , the initial population y_0 , and the saturation constant K .

The results for the three models are presented for *R. capsulatus* in Table 5.1 and for *C. vibrioforme* in Table 5.2. In both tables, “residual” is the value of the norm of the residual as defined above.

As expected the results of the curve fitting as measured with the “residual” are better for *R. capsulatus*, since the data points for *C. vibrioforme* deviate more from an exponential or an

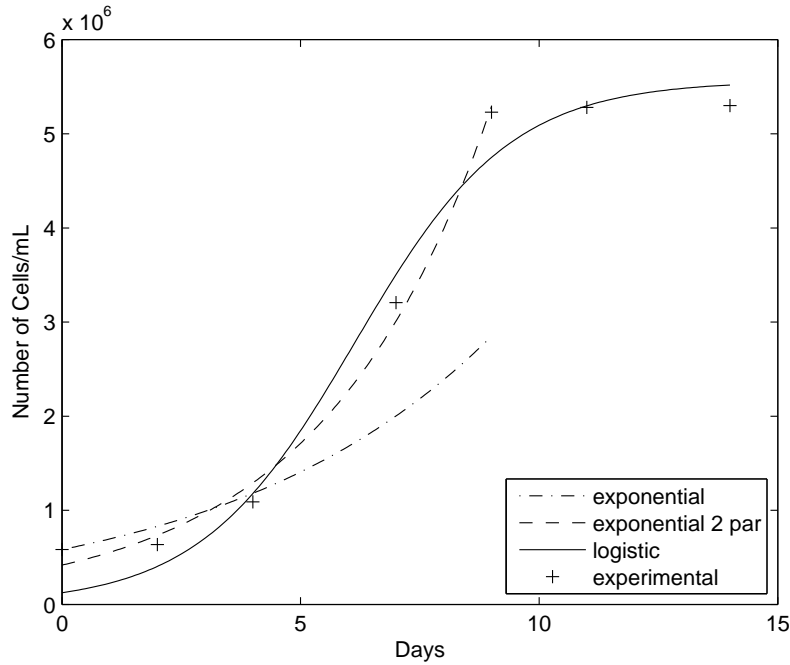


FIGURE 5.1. *The three growth models for R. capsulatus.*

“s-shaped” curve. The values of the fitted parameters depend significantly on the model used. In most population growth models, the value of r reported comes from fitting an exponential growth model. It is important to have multiple experiments to be able to take averages.

Figures 5.1 and 5.2 are plots of the three least squares fit curves together with the measured values. The figures show that the fitted curves approximate very well the experimental data, with the exception of Case I. This result is to be expected since we only have one parameter to fit to measurements that are very difficult to perform accurately. The curves for *R. capsulatus* fit better than those for *C. vibrioforme*, as expected.

5.2. Polynomial chaos. Figure 6.1 presents two results obtained by modeling the time evolution of the population of *R. capsulatus* using exponential growth. The polynomial chaos solution for the mean is shown together with two limit curves for the usual interval of confidence $[\bar{y}(t) - 2S(t), \bar{y}(t) + 2S(t)]$, where $S(t) = \sqrt{\text{Var}[y(t)]}$ is the standard deviation in the solution. Both computations use the same mean value of r obtained from Case II to allow comparison. For the top figure, only the growth rate is considered a Gaussian random variable. For the bottom figure, the initial value is also taken as a random variable, uniformly distributed in $(0.4074, 0.4274)$. Note the small values of the variances in the random coefficients; obviously introducing only a small randomness in the model inputs allows a more faithful representation of the time evolution of the population. For this reason, it is the authors’ opinion that the use of random coefficient differential equation models should be investigated more extensively in mathematical biology.

Figure 6.2 shows the evolution of the mean and the interval of confidence for the logistic model applied to *R. capsulatus*. The top figure only considers randomness in the growth rate (Gaussian) and the initial condition (uniform in $(0.0744, 0.1744)$). The bottom figure also takes into account randomness in the saturation level K (uniform in $(4.8, 6.32)$). It is

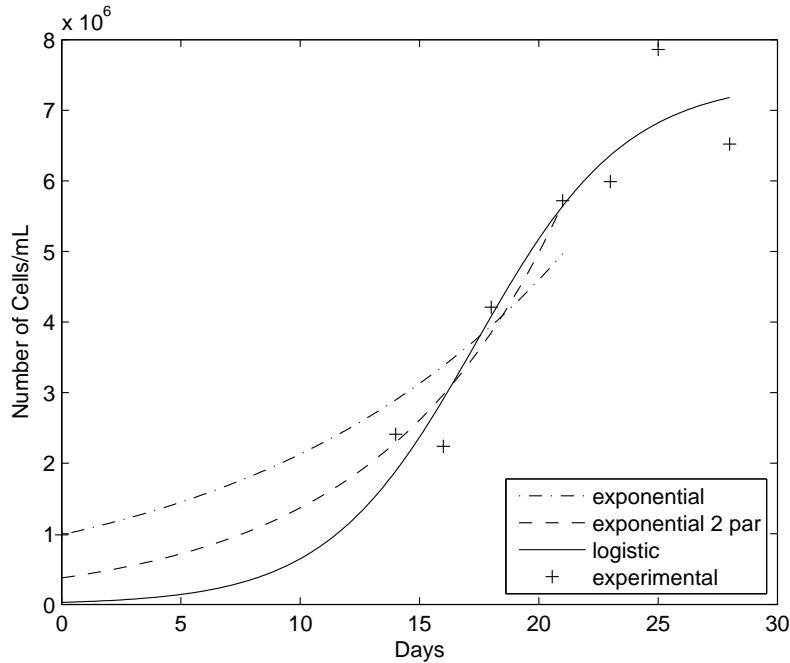


FIGURE 5.2. The three growth models for *C. vibrioforme*.

interesting to note the trend of the upper limit curve in the top figure. The increase continues beyond the saturation level, peaks, and only then starts decreasing toward the mean value of K . We have confirmed that with longer time integration, the upper and lower limits do join the mean as one would expect.

Figures 6.3 and 6.4 replicate these results for *C. vibrioforme*. In the top part of Figure 6.3, the initial value y_0 is set to the fitted value from Case II, and the growth rate is considered to have a normal distribution with the mean equal to the fitted value and $\text{Var}[r] = 0.03$. In the bottom plot, the variance of the growth rate is $\text{Var}[r] = 0.01$, but the initial value is uniformly distributed in $(0.3655, 0.3855)$. The logistic models with random coefficients shown in Figure 6.4 are similar to the results for *R. capsulatus*, except that the peak in the upper confidence limit does not appear. Although not shown here, we confirmed through longer time integration that the upper and lower confidence limit curves eventually join the mean value, as should be expected.

6. Conclusions. Modeling population growth is many times a difficult task due to the scarcity and scattering of the data, and to errors and uncertainty in it. Incorporating randomness in the population model is a natural alternative. In this paper, we have explored two classical population growth models which have been modified to take into account the randomness in the coefficients. While for very simple cases the exact solution for some of the moments may be computed analytically, the numerical alternative based on polynomial chaos that has been used here can be easily extended to take into account more difficult situations. Here we have used several different hypotheses on the distribution functions of the random coefficients. We have used actual data for two bacterial species growing under IR lighting conditions, and have calculated numerical solutions. The extension we envision is a random coefficient partial differential equations model for biofilm growth.

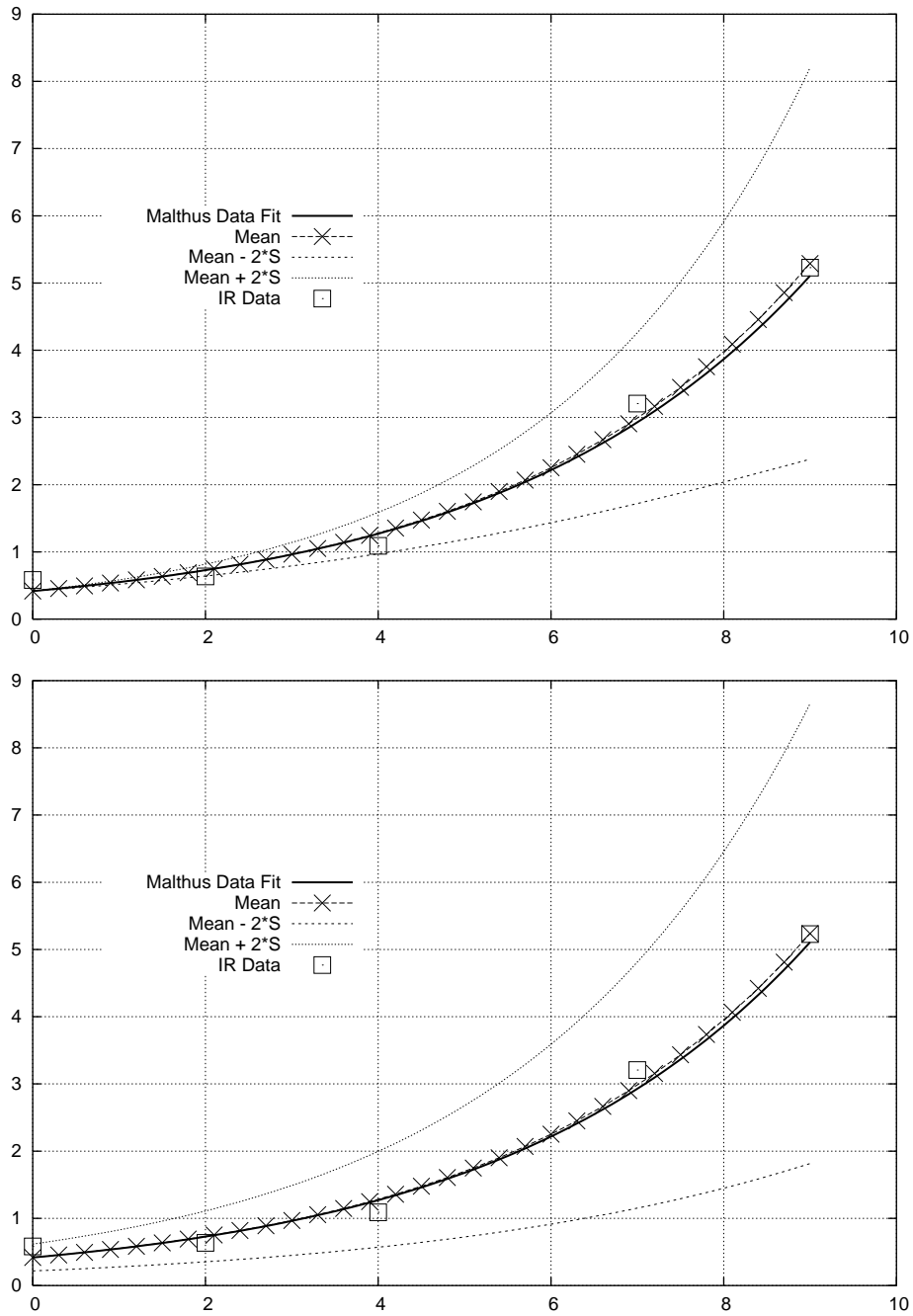


FIGURE 6.1. Modeling of *R. capsulatus* with exponential growth. Top figure: $\bar{r} = 0.2822$, $\text{Var}[r] = 0.03$, $\bar{y}_0 = 0.4174$, $\text{Var}[y_0] = 0$. Bottom figure: $\bar{r} = 0.2822$, $\text{Var}[r] = 0.01$, y_0 uniformly distributed in $(0.4074, 0.4274)$.

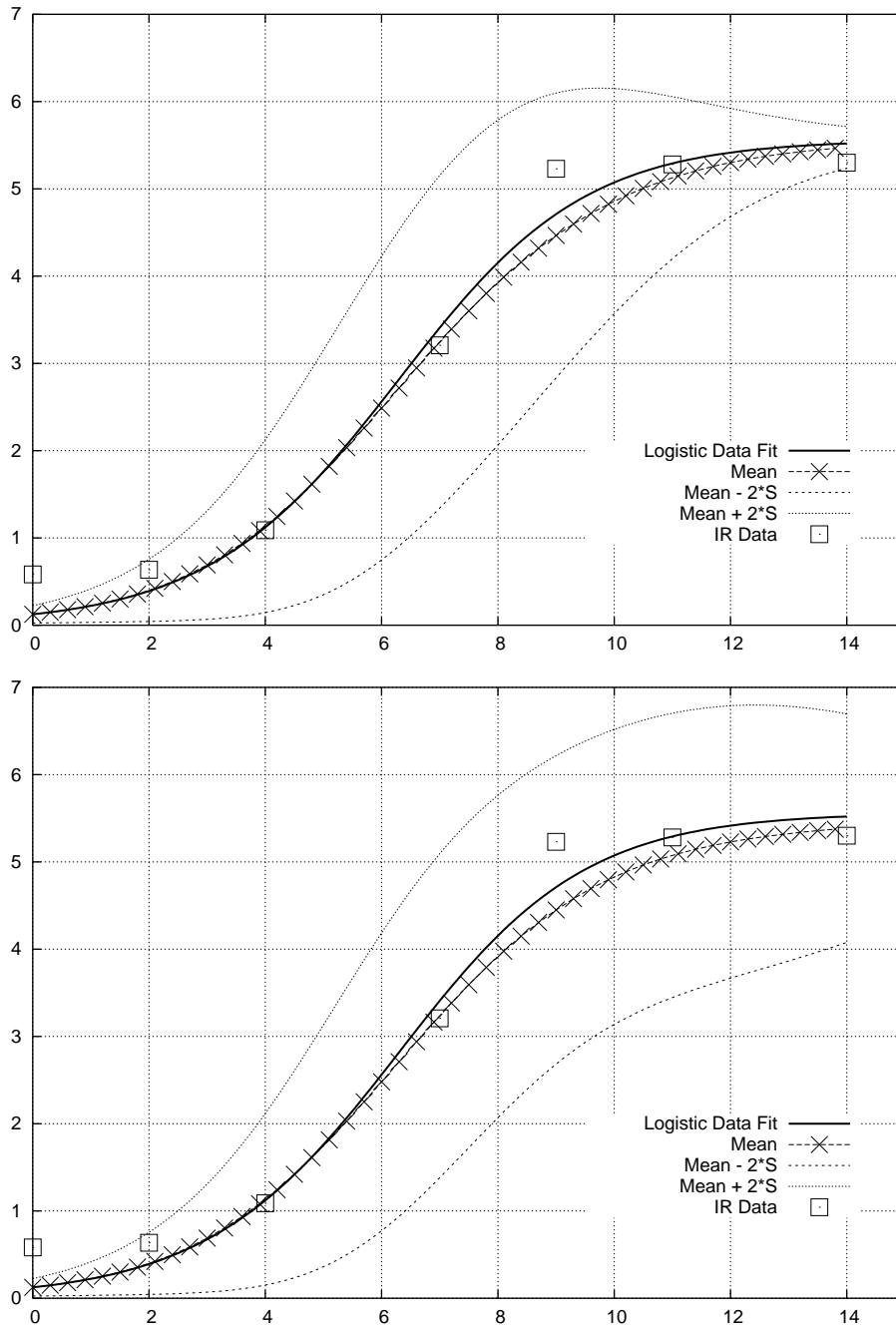


FIGURE 6.2. Modeling of *R. capsulatus* with logistic growth. Top figure: $\bar{r} = 0.6157$, $\text{Var}[r] = 0.04$, y_0 uniformly distributed in $(0.0744, 0.1744)$, $\bar{K} = 5.56$, $\text{Var}[K] = 0$. Bottom figure: r, y_0 same as for top figure, K uniformly distributed in $(4.8, 6.32)$.

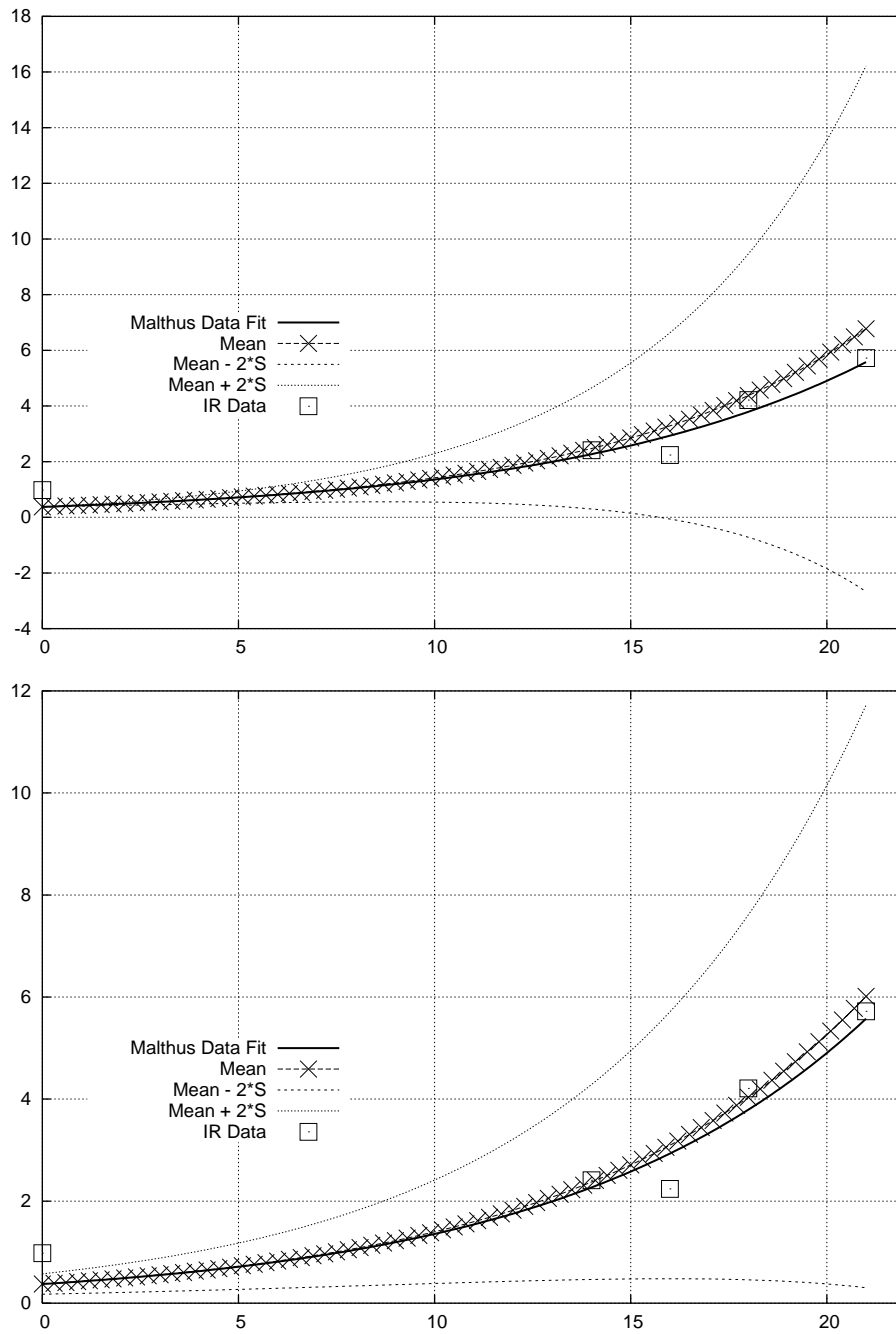


FIGURE 6.3. Modeling of *C. vibrioforme* with exponential growth. Top figure: $\bar{r} = 0.1293$, $\text{Var}[r] = 0.03$, $\bar{y}_0 = 0.3755$, $\text{Var}[y_0] = 0$. Bottom figure: $\bar{r} = 0.1293$, $\text{Var}[r] = 0.01$, y_0 uniformly distributed in $(0.3655, 0.3855)$.

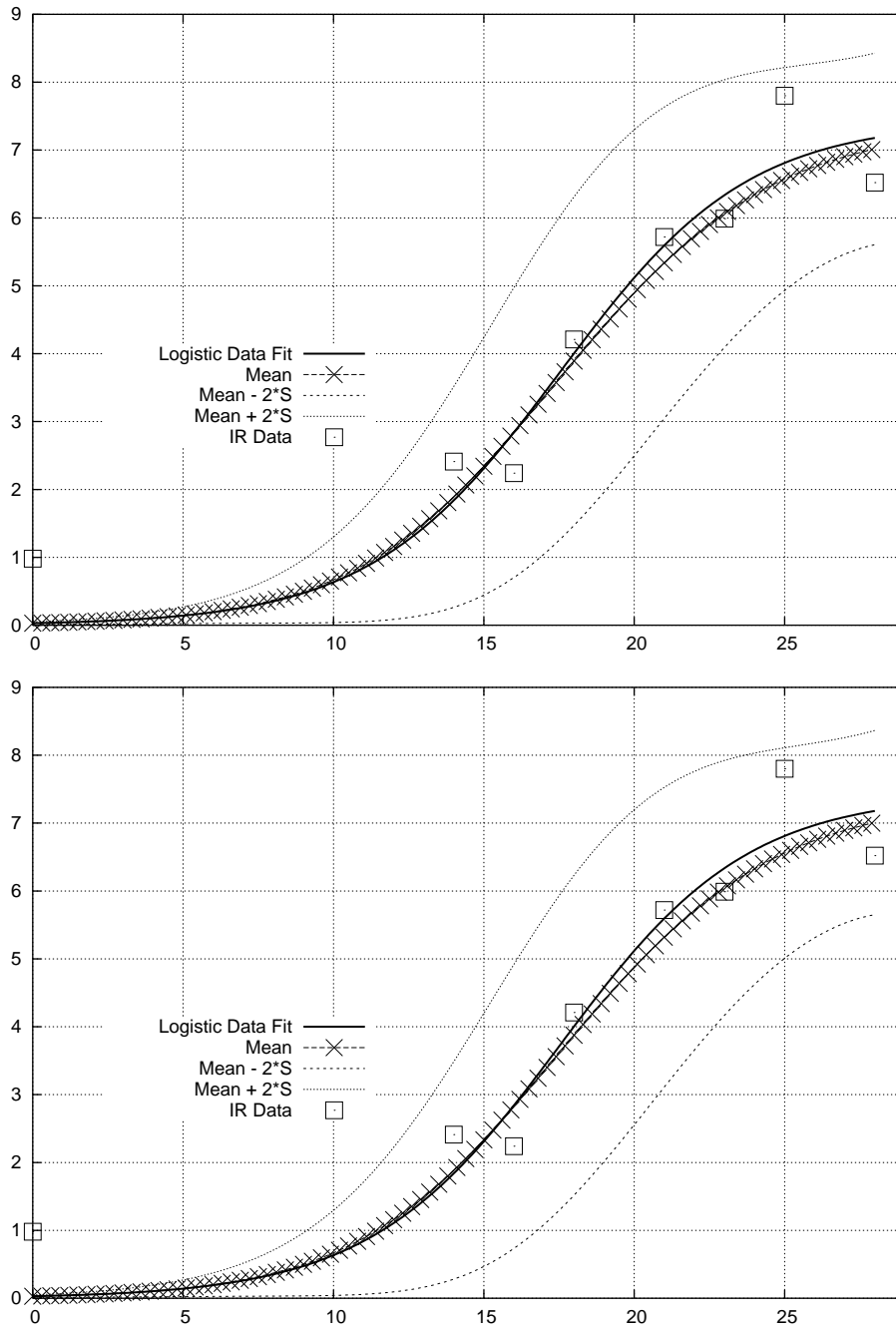


FIGURE 6.4. Modeling of *C. vibrioforme* with logistic growth. Top figure: $\bar{r} = 0.3184$, $\text{Var}[r] = 0.02$, y_0 uniformly distributed in $(0.02, 0.04)$, $\text{Var}[K] = 0$. Bottom figure: $\bar{r} = 0.3184$, $\text{Var}[r] = 0.01$, y_0 uniformly distributed in $(0.029, 0.031)$, K uniformly distributed in $(5.06, 6.06)$.

REFERENCES

- [1] R. CAMERON AND W. MARTIN, *The orthogonal development of nonlinear functionals in series of Fourier-Hermite functionals*, Ann. of Math., 48 (1947), pp. 385–392.
- [2] W. CHENEY AND D. KINCAID, *Numerical Mathematics and Computing*, fifth ed., Thomas Brooks/Cole, Belmont, California, 2004.
- [3] G. S. FISHMAN, *Monte Carlo: Concepts, Algorithms, and Applications*, Springer, New York, 1995.
- [4] R. GHANEM AND P. D. SPANOS, *Stochastic Finite Elements: a Spectral Approach*, Dover Publications, Mineola, New Jersey, 1991.
- [5] M. GRIGORIU AND T. SOONG, *Random Vibration of Mechanical and Structural Systems*, Prentice Hall, Englewood Cliffs, New Jersey, 1993.
- [6] G. KALLIANPUR, *Stochastic Filtering Theory*, Springer, Berlin, 1980.
- [7] I. KARATZAS AND S. E. SHREVE, *Brownian Motion and Stochastic Calculus*, Springer, Berlin, 1998.
- [8] J. KESSI, M. RAMUZ, E. WEHRLI, M. SPYCHER, AND R. BACHOFEN, *Reduction of selenite and detoxification of elemental selenium by the phototrophic bacterium Rhodospirillum rubrum*, Appl. Environ. Microbiol., 65 (1999), pp. 4734–4740.
- [9] J. R. LAWRENCE, D. R. KORBER, G. M. WOLFAARDT, D. E. CALDWELL, AND T. R. NEU, *Analytical imaging and microscopy techniques*, in Manual of Environmental Microbiology, C. J. Hurst, R. L. Crawford, G. R. Knudsen, M. K. McInerney, and L. D. Stetzenbach, eds., ASM Press, Washington, DC, 2002, pp. 52–53.
- [10] T. R. MALTHUS, *An Essay on the Principal of Population*, Oxford World’s Classics Paperbacks, Oxford University Press, Oxford, 1999.
- [11] N. METROPOLIS AND S. ULAM, *The Monte Carlo method*, J. Amer. Statist. Assoc., 44 (1949), pp. 335–341.
- [12] J. D. MURRAY, *Mathematical Biology I*, Springer, Berlin, 2002.
- [13] B. OKSENDAL, *Stochastic Differential Equations*, sixth ed., Springer, Heidelberg, 2003.
- [14] S. ROSS, *A First Course in Probability*, Prentice Hall, Englewood Cliffs, New Jersey, 2002.
- [15] W. R. SISTROM, *A requirement for sodium in the growth of Rhodopseudomonas sphaeroides*, J. Gen. Microbiol., 22 (1960), pp. 778–785.
- [16] T. SOONG, *Random Differential Equations in Science and Engineering*, Academic Press, New York, 1973.
- [17] ———, *Probabilistic Modeling and Analysis in Science and Engineering*, Wiley, New York, 1992.
- [18] P. F. VERHULST, *Notice sur la loi que la population suit dans son accroissement*, Corr. Math. et Phys., 10 (1838), pp. 113–121.
- [19] L. VILLAFUERTE, *Numerical and Analytical Mean Square Solutions for Random Differential Models*, Ph.D. thesis, Department of Applied Mathematics, Valencia Polytechnic University, 2007.
- [20] R. W. WALTERS AND L. HUYSE, *Uncertainty quantification for fluid mechanics with applications*, Tech. Report ICASE Report No. 2002-1, NASA Langley Research Center, Hampton, Virginia, 2002.
- [21] N. WIENER, *The homogeneous chaos*, Amer. J. Math., 60 (1938), pp. 897–936.
- [22] D. XIU AND G. E. KARNIADAKIS, *The Wiener-Askey polynomial chaos for stochastic differential equations*, SIAM J. Sci. Comput., 24 (2002), pp. 619–664.